

Topological “Shape” in Micellar Dynamics

Thomas J. Peters,* Kirk E. Jordan, Ji Li, Kirk Gardner, Breannan Ó. Conchúir, William C. Swope, Vassilis Vassiliadis, Michael A. Johnston, and Peter Zaffetti



Cite This: *ACS Omega* 2024, 9, 16084–16088



Read Online

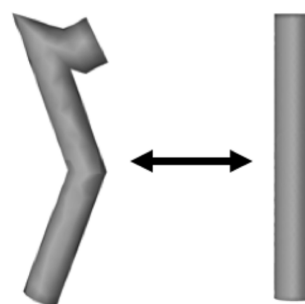
ACCESS |

Metrics & More

Article Recommendations

ABSTRACT: For micelles, “shape” is prominent in rheological computations of fluid flow, but this “shape” is often expressed too informally to be useful for rigorous analyses. We formalize topological “shape equivalence” of micelles, both *globally* and *locally*, to enable visualization of computational fluid dynamics. Although topological methods in visualization provide significant insights into fluid flows, this opportunity has been limited by the known difficulties in creating representative geometry. We present an agile geometric algorithm to represent the micellar shape for input into fluid flow visualizations. We show that worm-like and cylindrical micelles have formally equivalent shapes, but that visualization accentuates unexplored differences. This *global–local* paradigm is extensible beyond micelles.

Topological Shape Equivalence for Micelles



1. INTRODUCTION: FORMALIZING THE CHEMICAL SHAPE

To envision the role of “shape” for fluid flow about a micelle,^{1,2} consider Figure 1 for the cylinder, C , and Figure 2 for a worm-like micelle (WLM), denoted by $\Delta(\Lambda(\kappa))$. Previous tractable rheology calculations simplified “shape” to long cylinders,³ which is topologically consistent with WLMs emerging from cylinders during molecular simulations.⁴ However, Figures 1 and 2 exhibit differences in their vector fields, contrasting flow curves that are primarily linear versus those with noticeable nonlinearity (the colors indicate speed which depends on the cross section of the object, a geometric parameter which is ignored here.) Further investigation by topological methods for visualization^{5,6} requires a formal representation of the “shape” of a micelle, with contributions here, *globally* by isotopy^{7a} and *locally* by curvature.⁹

Our Figures 1 and 2 represent instantaneous frames of a synchronous visualization of a molecular simulation,⁴ showing a micelle under laminar flow within a containing cylinder.

2. RELATED WORK

Topology is prominent in chemistry^{10–12}—notably knot theory.⁷ Ambient isotopy is the equivalence relation in knot theory and is applied in computational geometry.¹³ The formulation of simplified rheological calculations using long cylinders³ is consistent with ambient isotopic equivalence between WLMs and cylinders. Topological methods for temporal changes across frames^{5,6} appear appropriate to investigate the flow differences shown between Figures 1 and 2.

Previous data and simulation results⁴ were used in the present work. Some of the current authors created topological methods to visualize¹⁴ knotted proteins as 1-manifolds.^{7,8} Topology formalisms were not explicated in other shape-based computations.^{3,15,16}

The visualizations available from computational fluid dynamics (CFD) software^{1,2} are integral to a comprehensive workflow.¹⁷ Quantitative consideration of shape appears broadly in chemistry.^{18–21} Shape modeling is pervasive in fluid analyses in science, engineering,^{5,6} and athletics.^{22,23b}

3. RESULTS AND DISCUSSION

In the following three subsections, we formalize intuition for WLMs by presenting:

- a proof of isotopy to cylinders (Section 3.1)
- a geometric algorithm (Section 3.2, Algorithm 1) and
- an example of inequivalence (Section 3.3).

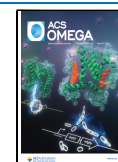
3.1. Global Equivalence of Isotopy for WLMs. The *global* shape equivalence of ambient isotopy^{7,8,13,24} is chosen, as “...a homotopy of homeomorphisms...”⁸ (see Definition 3.0 below.) We avoid the numeric calculations inherent in shape *quantification*,^{18–21} providing a more abstract overview for

Received: December 6, 2023

Revised: March 1, 2024

Accepted: March 6, 2024

Published: March 29, 2024



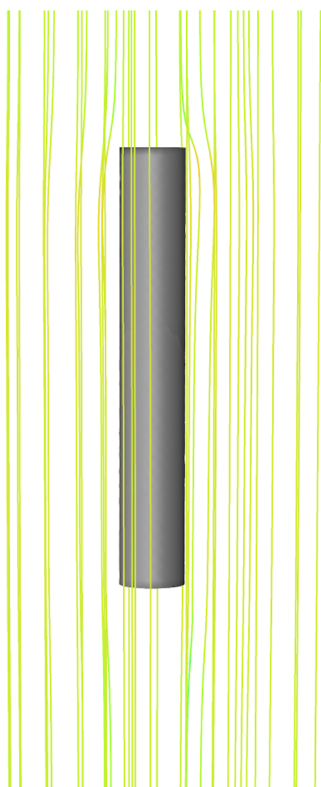


Figure 1. Flow over the cylinder, C .

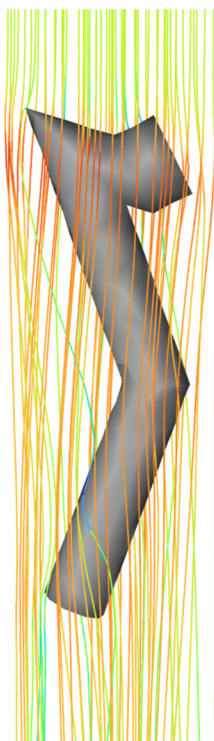


Figure 2. Flow over the WLM, $\Delta(\Lambda(\kappa))$.

refinement.^{5,6} Our dimensional extension from 1-manifolds¹⁴ to 3-manifolds is significant, as presented in Lemma 3.2.

Figures 3 and 4 illustrate a WLM as a union of subsets of a cylinder,⁴ as formalized in Algorithm 1. The black dots in Figure 3 depict the 3D coordinates of point cloud data of atom centers,



Figure 3. Skeleton κ and 3-manifold $\Lambda(\kappa)$.

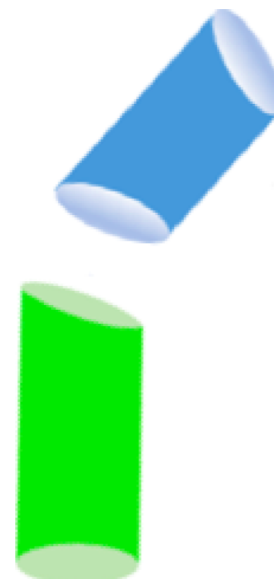


Figure 4. Zoomed view of the lowest cut.

used to produce the 3-manifold $\Lambda(\kappa)$ and its approximation, $\Delta(\Lambda(\kappa))$ of Figure 2. There are no self-intersections.⁴

Figure 4 is a zoomed, exploded view of the 2 lowest sections of Figure 3. Abstractly, the circular stock is cut into subsets. The first cut is by a plane containing the vertex v_1 so that the cut pieces can be repositioned and joined at an angle bisecting α_1 . These cuts share an elliptical cross-section. The process continues until the final angle α_m is bisected for a union that is a 3-manifold (with boundary),^{7,8} denoted by $\Lambda(\kappa)$.

Definition 3.0: Let X and Y be two subspaces of \mathbb{R}^3 . A continuous function

$$\mathcal{H}: \mathbb{R}^3 \times [0, 1] \rightarrow \mathbb{R}^3$$

is an **ambient isotopy** between X and Y if $H(\cdot, 0)$ is the identity, $H(X, 1) = Y$, and $\forall t \in [0, 1]$, $H(\mathbb{R}^3, t)$ is a homeomorphism onto \mathbb{R}^3 .

Let C denote a solid, right circular cylinder [a 3-manifold (with boundary)^{7,8}]. Let κ denote a skeletal 1-manifold and $\Lambda(\kappa)$ denote the corresponding 3-manifold (with boundary) previously described,⁴ as shown in Figures 3 and 4, with geometric construction now formalized in Algorithm 1.

The skeletal κ is represented as a piecewise linear (PL) curve, defined by finitely many, unique, ordered vertices, denoted by v_i and line segments between consecutive vertices, denoted by l_i . The l_i are pairwise disjoint, except at the vertex shared by consecutive segments. The angles between consecutive segments^c are denoted by α_i . The boundary curves created at the v_i are parametrized over $[0,1]$ for successive approximations during the workflow.¹⁷ The value of a radius r was chosen^d so that $\Lambda(\kappa)$ is a 3-manifold for a WLM.

Lemma 3.1: The PL 1-manifold for a WLM skeleton is ambient isotopic to $[0,1]$.

Proof: The proof is shown by induction. For $m \geq 1$, let κ_m denote the PL curve for the WLM skeleton of m segments. The base case of $m = 1$ is trivial.

Induction Hypothesis: There exists $m \geq 1$ with κ_m ambient isotopic to $[0,1]$. With l_{m+1} as the terminal segment of κ_{m+1} , let $\mathcal{T}(l_{m+1})$ be a tetrahedral neighborhood of l_{m+1} , with $\mathcal{T}(l_{m+1}) \cap \kappa_m = v_m$, $v_m \in \partial\mathcal{T}(l_{m+1})$, and $l_{m+1} - v_m \subset \text{int}\mathcal{T}(l_{m+1})$.

Using $\mathcal{T}(l_{m+1})$ as compact support,²⁵ isotopically contract l_{m+1} to l_{m+1}^* with a sufficiently small nonzero length such that another neighborhood $\mathcal{T}(l_{m+1}^* \cup l_m)$ is compact support for an isotopy of κ_{m+1} to κ_m , where $\mathcal{T}(l_{m+1}^* \cup l_m) \cap \kappa_m = l_m$ and $l_{m+1}^* \cup (l_m - v_{m-1}) \subset \text{int}\mathcal{T}(l_{m+1}^* \cup l_m)$.

Apply the Induction Hypothesis.

Lemma 3.2: The 3-manifold $\Lambda(\kappa)$ is ambient isotopic to C .

Proof: Extend the proof of Lemma 3.1.

For input to CFD code, our PL ambient isotopic approximations of WLMs in Algorithm 1 follow the principles of the Simulation Toolkit for Scientific Discovery.¹⁷

Corollary 3.3: By appropriate partitioning of $[0,1]$, there are PL approximations of $\Lambda(\kappa)$, denoted by $\Delta(\Lambda(\kappa))$, that are ambient isotopic to $\Lambda(\kappa)$ and to C .

3.2. Local WLM Curvature: Algorithm 1. The prior isotopic equivalence narrowed our algorithm design to specialized geometry for WLMs. We restricted attention to planar-cylinder intersections for simplicity²⁶ to avoid “...the typical obstacles in construction and meshing...”¹⁵ inclusive of pernicious numeric issues.²⁷ The resultant workflow agility¹⁷ is formalized by Corollary 3.3. The impact of Algorithm 1 is that agile, specialized geometric algorithms can be designed for broader use of CFD for micelles.

Our Algorithm 1 represents local curvature^{8,9,27} to extend beyond previous geometric models.^{3,4} In Figure 3, the defining skeleton, κ , is the central PL curve, defined by finitely many consecutive, unique vertices, denoted by v_0, v_1, \dots, v_m with angles $\alpha_1, \dots, \alpha_m$ between consecutive linear segments. These joining angles approximate the local Gaussian curvature.^{4,9}

The notation for a skeleton,⁴ κ , is summarized as:

- v_0, v_1, \dots, v_m the unique, ordered vertices,
- l_1, \dots, l_m the connecting segments, and
- $\alpha_1, \dots, \alpha_m$ the angles between segments.

Algorithm 1: 3-manifold Model for a WLM⁴

Input: A skeleton, κ of a WLM and
the radius, r , for $\Lambda(\kappa)$ to be nonselfintersecting.

Output: The 3-manifold model, $\Lambda(\kappa)$.

1. **INITIALIZE** the Circular Stock Pieces: d

FOR $i = 1, \dots, m$,

Let C_i be the right circular cylinder

of radius r , axis l_i .

ENDFOR

2. Let \mathcal{H}_0 be the half-space

(a) containing v_0 and v_1 and

(b) having normal, \vec{n}_0 , collinear with l_1 .

3. **FOR** $i = 1, \dots, m$,

(a) Let \mathcal{H}_i be the half-space

- containing v_{i-1} and v_i ,

- having a bounding plane, Π_i , that

- i. contains v_i and

- ii. bisects the angle α_i .

(b) Let $\Lambda_i(\kappa) = C_i \cap \mathcal{H}_i \cap \mathcal{H}_{i-1}$.

ENDFOR

4. Let $\Lambda(\kappa) = \bigcup_{i=1}^m \Lambda_i(\kappa)$.

5. **END**

Algorithm 1 produces micellar geometry with approximations of the local Gaussian curvature for input to CFD.²⁸ Our synthesized geometry was created by invoking Algorithm 1 with available software.^{1,2}

3.3. Global Shape Inequivalence to a Cylinder. Figure 5 is a branched micelle,⁴ denoted as B . The 3-manifolds B and C are not homeomorphic,⁷ hence not isotopic. Recent work on branched micelles²⁹ underscores the timeliness of the following question.

3.3.1. Despite This Global Shape Inequivalence to C , Is B Admissible Input for CFD Analyses? We answer “Yes” after constructing a geometric representation of this branched micelle. The vector field for fluid flow in Figure 5 differs from the previous visualizations—an opportunity to consider behavior over inequivalent shape classes.^{5,6} This classification approach is extensible to branched micelles of different isotopy

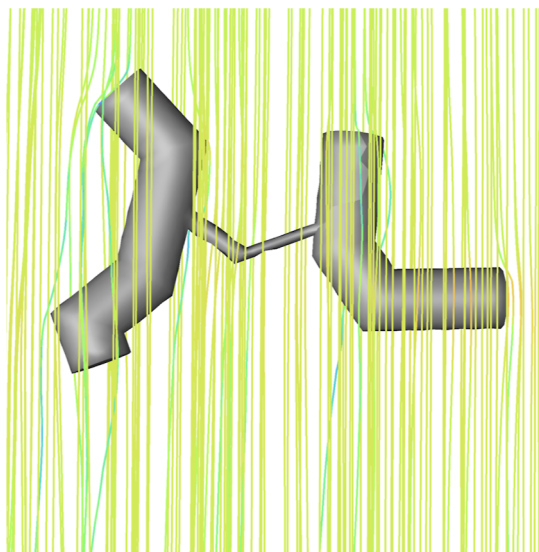


Figure 5. Flow over the branched micelle, *B*.

equivalence classes,²⁹ depending upon creation of appropriate geometric representations.

Our *Branched Micelle Construction* adapts and extends the use of Algorithm 1 for applications beyond WLMs. We present notation for geometric subsets of *B* from Figure 5, expecting the correspondence to be intuitively obvious to the reader. Each subset is visually similar to a WLM, denoted as:

- *L* for the *left* branch,
- *M* for the *middle* narrow bridge, and
- *R* for the *right* branch.

The modeling operation of “join” over regular closed sets^{27,30} is denoted here by “ \vee ”.

Branched Micelle Construction.

Input: *L*, *M*, *R*,

Output: *B*.

$$B = L \vee M \vee R$$

This use of “ \vee ” depends on a cylinder–cylinder intersection, which can introduce subtleties.^{31–33} Pragmatically, those subtleties were avoided here by user expertise so that any broad adaptation of this approach remains a subject of further investigation.

4. CONCLUSIONS AND FUTURE WORK

We present a promising *proof of concept* for formalizing “*shape*” in rheological analyses by rigorous application of topology and geometry. This novel theoretical approach supports the creation of innovative micellar models for CFD input. These micellar models:

- preserve *global* shape equivalence and
- approximate the *local* Gaussian curvature.

The micelles that are cylindrical and worm-like share a formal shape equivalence by ambient isotopy, but the distinct differential topology properties for fluid flow remain to be investigated by methods from topological visualization. The shapes of branched micelles are shown to be a formally separate topological class. Three examples were constructed with a creative algorithm presented here that requires minimal software implementation by reliance on available geometric tools.

Verification of sufficient geometric coverage is relegated to future work.

Our new “*shape*” paradigm for micelles can be extended by additional data-specific algorithms for geometry creation. A direct geometric interface between the HPC simulation and the CFD software presents a formidable engineering task as a long-term goal.

■ AUTHOR INFORMATION

Corresponding Author

Thomas J. Peters – Department of Computer Science and Engineering, 371 Fairfield Way, University of Connecticut, Storrs, Connecticut 06269, United States; orcid.org/0000-0003-0835-6696; Email: tjp5k82@gmail.com

Authors

Kirk E. Jordan – IBM Research, Cambridge, Massachusetts 02141, United States

Ji Li – Department of Computer Science and Engineering, 371 Fairfield Way, University of Connecticut, Storrs, Connecticut 06269, United States

Kirk Gardner – Department of Computer Science and Engineering, 371 Fairfield Way, University of Connecticut, Storrs, Connecticut 06269, United States

Breannan Ó. Conchúir – IBM Research Europe, Daresbury WA4 4AD, U.K.; orcid.org/0000-0002-4667-8402

William C. Swope – IBM Research, San Jose, California 95120, United States; orcid.org/0000-0002-5299-4145

Vassilis Vassiliadis – IBM Research Europe, Dublin 15 D15 HN66, Ireland

Michael A. Johnston – IBM Research Europe, Dublin 15 D15 HN66, Ireland

Peter Zaffetti – Department of Computer Science and Engineering, 371 Fairfield Way, University of Connecticut, Storrs, Connecticut 06269, United States

Complete contact information is available at:

<https://pubs.acs.org/10.1021/acsomega.3c09754>

Notes

The authors declare no competing financial interest.

■ ACKNOWLEDGMENTS

Authors T.J.P. and K.G. acknowledge, with appreciation, the generous financial support provided by IBM Research, under award IBM-TJP-6328340. All statements made here are the responsibility of the authors, *not* of IBM. This work was also supported by the Hartree National Centre for Digital Innovation, a collaboration between STFC and IBM. The authors thank the reviewers for many helpful comments, including some relevant citations.

■ ADDITIONAL NOTES

^aAmbient isotopy is also a classical concept.⁸

^bCyclists and skiers “tuck” to reduce drag.

^cThe number of segments is one less than the number of vertices, as also holds for the number of angles.

^dThis algorithm is *not directly* applicable to branched micelles, but adaptations are given in Section 3.3.

■ REFERENCES

(1) Ansys SpaceClaim, 3D Modeling Software. 2022; <https://www.ansys.com/products/3d-design/ansys-spaceclaim>.

- (2) Ansys Fluent (Version 2022 R1 Student). 2022; <https://www.ansys.com/products/fluids/ansys-fluent>.
- (3) Dutta, S.; Graham, M. D. Mechanistic constitutive model for wormlike micelle solutions with flow-induced structure formation. *J. Non-Newtonian Fluid Mech.* **2018**, *251*, 97–106.
- (4) Conchuir, B. O.; Gardner, K.; Jordan, K. E.; Bray, D. J.; Anderson, R. L.; Johnston, M. A.; Swope, W. C.; Harrison, A.; Sheehy, D. R.; Peters, T. J. Efficient Algorithm for the Topological Characterization of Worm-like and Branched Micelle Structures from Simulations. *J. Chem. Theory Comput.* **2020**, *16*, 4588–4598.
- (5) Hauser, H.; Hagen, H.; Theisel, H. *Topology-Based Methods in Visualization*; Springer Science & Business Media, 2007.
- (6) Pascucci, V.; Tricoche, X.; Hagen, H.; Tierny, J. *Topological Methods in Data Analysis and Visualization: Theory, Algorithms, and Applications*; Springer Science & Business Media, 2010.
- (7) Ghrist, R. *Elementary Applied Topology*; CreateSpace Independent Publishing Platform, 2014.
- (8) Hirsch, M. W. *Differential Topology*; Springer: New York, 1976.
- (9) Farin, G. *Curves and Surfaces for Computer Aided Geometric Design*; Academic Press: San Diego, CA, 1990.
- (10) Polya, G.; Read, R. C. *Combinatorial Enumeration of Groups, Graphs, and Chemical Compounds*; Springer Science & Business Media, 2012.
- (11) Sumners, D. W. Untangling DNA. *Math. Intel.* **1990**, *12*, 71–80.
- (12) Wasserman, E. Chemical topology. *Sci. Am.* **1962**, *207*, 94–102.
- (13) Amenta, N.; Peters, T. J.; Russell, A. C. Computational topology: Ambient isotopic approximation of 2-manifolds. *Theor. Comput. Sci.* **2003**, *305*, 3–15.
- (14) Jordan, K. E.; Miller, L. E.; Peters, T. J.; Russell, A. C. Geometric topology & visualizing 1-manifolds. *Topological Methods in Data Analysis and Visualization: Theory, Algorithms, and Applications*; Springer Science & Business Media, 2011; Vol. 1–12.
- (15) Kalli, M.; Pico, P.; Chagot, L.; Kahouadji, L.; Shin, S.; Chergui, J.; Juric, D.; Matar, O.; Angeli, P. Effect of surfactants during drop formation in a microfluidic channel: a combined experimental and computational fluid dynamics approach. *J. Fluid Mech.* **2023**, *961*, A15.
- (16) Padding, J. T.; Boek, E. S.; Briels, W. J. Dynamics and rheology of wormlike micelles emerging from particulate computer simulations. *J. Chem. Phys.* **2008**, *129*, 074903.
- (17) Johnston, M. A.; Vassiliadis, V. Towards an Approximation-Aware Computational Workflow Framework for Accelerating Large-Scale Discovery Tasks. *ACM ApPLIED* **2022**, 7–14.
- (18) Chremos, A.; Horkay, F.; Douglas, J. F. Influence of network defects on the conformational structure of nanogel particles: From “closed compact” to “open fractal” nanogel particles. *J. Chem. Phys.* **2022**, *156*, 156.
- (19) Mansfield, M. L.; Douglas, J. F. Shape characteristics of equilibrium and non-equilibrium fractal clusters. *J. Chem. Phys.* **2013**, *139*, 044901.
- (20) Vargas-Lara, F.; Hassan, A. M.; Mansfield, M. L.; Douglas, J. F. Knot energy, complexity, and mobility of knotted polymers. *Sci. Rep.* **2017**, *7*, 13374.
- (21) Vargas-Lara, F.; Starr, F. W.; Douglas, J. F. Solution properties of spherical gold nanoparticles with grafted DNA chains from simulation and theory. *Nanoscale Adv.* **2022**, *4*, 4144–4161.
- (22) Blocken, B.; van Druenen, T.; Toparlar, Y.; Andrienne, T. CFD analysis of an exceptional cyclist sprint position. *Sports Eng.* **2019**, *22*, 10–11.
- (23) Elfmark, O.; Teigen Giljarhus, K. E.; Liland, F. F.; Oggiano, L.; Reid, R. Aerodynamic investigation of tucked positions in alpine skiing. *J. Biomech.* **2021**, *119*, 110327.
- (24) Bing, R. H. *The Geometric Topology of 3-Manifolds*; American Mathematical Society: Providence, RI, 1983.
- (25) Andersson, L. E.; Dorney, S.; Peters, T.; Stewart, N. Polyhedral perturbations that preserve topological form. *Comput. Aided Geomet. Des.* **1995**, *12* (8), 785–799.
- (26) Requicha, A. A.; Rossignac, J. R. Solid modeling and beyond. *IEEE Comput. Graph. Appl. Mag.* **1992**, *12*, 31–44.
- (27) Hoffmann, C. M. *Geometric and Solid Modeling: an Introduction*; Morgan Kaufmann Publishers Inc., 1989.
- (28) Meshing-Roundtable Amsterdam, 2023. <https://internationalmeshingroundtable.com/papers/> (accessed November 17, 2023).
- (29) Zou, W.; Tan, G.; Weaver, M.; Koenig, P.; Larson, R. G. Mesoscopic modeling of the effect of branching on the viscoelasticity of entangled wormlike micellar solutions. *Phys. Rev. Res.* **2023**, *5*, 043024.
- (30) Tilove, R.; Requicha, A. A. Closure of boolean operations on geometric entities. *Comput. Aided Des.* **1980**, *12*, 219–220.
- (31) Hu, C.-Y.; Patrikalakis, N. M.; Ye, X. Robust interval solid modelling part I: representations. *Comput. Aided Des.* **1996**, *28*, 807–817.
- (32) Peters, T.; Bisceglia, J.; Ferguson, D.; Hoffmann, C.; Maekawa, T.; Patrikalakis, N.; Sakkalis, T.; Stewart, N. Computational topology for regular closed sets (within the I-TANGO project). *Topol. Atlas Invited Contrib.* **2004**, *9*, 12.
- (33) Patrikalakis, N. M.; Prakash, P. V. Surface-to-surface intersections for geometric modeling. *J. Mech. Des. Mar.* **1990**, *112*, 100.